

## Equations and Nomogram for the Relationship of Human Blood $p_{50}$ to 2,3-Diphosphoglycerate, $\text{CO}_2$ , and $\text{H}^+$

Michele Samaja,<sup>1</sup> Andrea Mosca,<sup>2</sup> Massimo Luzzana,<sup>2</sup> Luigi Rossi-Bernardi,<sup>2</sup> and Robert M. Winslow<sup>3</sup>

We describe a new method for tonometry of small amounts of blood (up to 0.25 mL) at known  $p_{\text{O}_2}$ ,  $p_{\text{CO}_2}$ , and temperature, in small, reusable, closed Pyrex flasks. Equilibrated blood is analyzed for oxygen saturation, pH, and organic phosphate concentration with standard techniques, and its  $p_{50}$  (the  $p_{\text{O}_2}$  at which hemoglobin is half-saturated with oxygen) is determined with full control of all the variables known to affect it. The SD in the measurement of  $p_{50}$  is 0.044 kPa (0.33 mmHg). We made 63 determinations of  $p_{50}$  on normal human blood under different conditions of pH and  $p_{\text{CO}_2}$ , and with different concentrations of 2,3-diphosphoglycerate and ATP. Empirical equations and a nomogram were derived, which allow the calculation of  $p_{50}$  from known values of  $p_{\text{CO}_2}$ , pH, and  $[\text{2,3-DPG}]/[\text{Hb}_4]$  molar ratio with a SD of 97 and 114 Pa (0.73 and 0.86 mmHg), respectively.

**Additional Keyphrases:** blood gases • phosphate • tonometry

The accurate and reproducible determination of  $p_{50}$  (the  $p_{\text{O}_2}$  at which hemoglobin is half-saturated with oxygen) is of great importance in physiological and clinical practice. It is well known that, under physiological conditions, the value of  $p_{50}$  is mainly determined by the concentration of  $\text{CO}_2$ , hydrogen ions, and organic phosphates in the erythrocyte. An integrated analysis of the reciprocal influence of such allosteric effectors on the oxygen affinity of whole, normal human blood is still lacking. Since the early work of Severinghaus (1), who introduced a blood gas calculator to obtain  $p_{50}$  from  $p_{\text{O}_2}$  and oxygen saturation ( $s_{\text{O}_2}$ ) at the  $p_{\text{CO}_2}$  of 40 mmHg,<sup>4</sup> other workers have proposed equations or nomograms for the same purpose (2-4). None of them, however, took into account the concentration of organic phosphates, which strongly affect the reaction of hemoglobin with oxygen.

In a previous paper Musetti et al. (5) constructed a nomogram that required knowledge of the concentration of 2,3-diphosphoglycerate (2,3-DPG) for the estimation of  $p_{50}$ . Only molar ratios of  $[\text{2,3-DPG}]$  to  $[\text{Hb}_4]$  of less than 1 were investigated in this preliminary work; however, it is now known that in many instances (pyruvate kinase deficiency, high-altitude acclimatization, chronic and acute pulmonary disease) concentrations of 2,3-DPG may be higher.

The aims of the present work are: (a) to propose a new time-saving and accurate method for determination of  $p_{50}$ , which requires very small volumes of blood (up to 0.25 mL);

and (b) to describe a nomogram and some empirical equations that allow estimation of  $p_{50}$  from known pH,  $p_{\text{CO}_2}$ , and  $[\text{2,3-DPG}]/[\text{Hb}_4]$  molar ratio.

### Materials and Methods

**Tonometric flasks.** The main innovative feature of this method is the closed tonometry system with the anaerobic flasks shown in Figure 1. We used two different flasks. The sample capacity of the smaller flask (a) is 0.25 mL of sample, that of the larger one (b) about 0.4 mL. Both are hand-blown, reusable Pyrex flasks and are anaerobically sealed with Neoprene septa and aluminum seals with tear tabs on the top to expose the puncturing area. Aluminum seals are applied to the flasks with a hand crimper.

**Tonometer.** The tonometer (Figure 2) is an aluminum block with provision for insertion of four flasks. An all-solid-state heating element and a control circuit (not shown in the figure) keep the temperature of the flasks at 37 °C (SD 0.1 °C). A motor (not shown) positions the block upwards for loading and unloading flasks, or reclined at 90° for tonometry. A second motor rotates the flasks at 7 rpm, allowing the sample to form a thin boundary on the inner surface, thus accelerating its equilibration with the appropriate gas.

**Equilibrating gas.** Cylinders containing the binary gas mixture of certified composition ( $\text{CO}_2$  concentrations: 3.1, 6.2, and 12.0 mL/100 mL, the rest being air or nitrogen), double-stage SOITAA 2UNI 4401 pressure regulators, and the two precision Sho-Rate Brooks flowmeters were purchased from SIAD, Milan, Italy. Connection tubings are of the high-vacuum type (5-mm wall thickness). All joints are firmly held together by leak-proof fittings. The oxygen content in the gas is measured by a type OA 273 oxygen analyzer (Taylor Servomex Ltd., Crowborough, Sussex, U.K.), which is calibrated by alternately passing through it oxygen-free nitrogen and air,

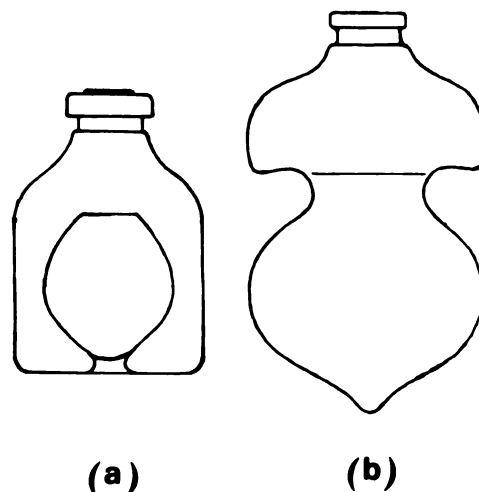


Fig. 1. Tonometry flasks (a) 46 mm (o.d.)  $\times$  49 mm (height) flask, volume 43 mL, volume of sample 0.25 mL; (b) 43 mm (o.d.)  $\times$  81 mm (height) flask, volume 56 mL, volume of sample 0.4 mL.

<sup>1</sup> Centro di Fisiologia del Lavoro Muscolare del CNR, Via Mangiagalli 32, 20133 Milan, Italy.

<sup>2</sup> Cattedra di Chimica Biologica V, Department of Medicine, and Ospedale San Raffaele, University of Milan, Milan, Italy.

<sup>3</sup> Hematology Division, Centers for Disease Control, 1600 Clifton Road, N.E., Atlanta, GA 30333 (address for correspondence and reprint requests).

<sup>4</sup> 1 mmHg = 133 Pa (the SI unit, which is not yet in common use in clinical laboratories).

Received Apr. 17, 1981; accepted July 30, 1981.

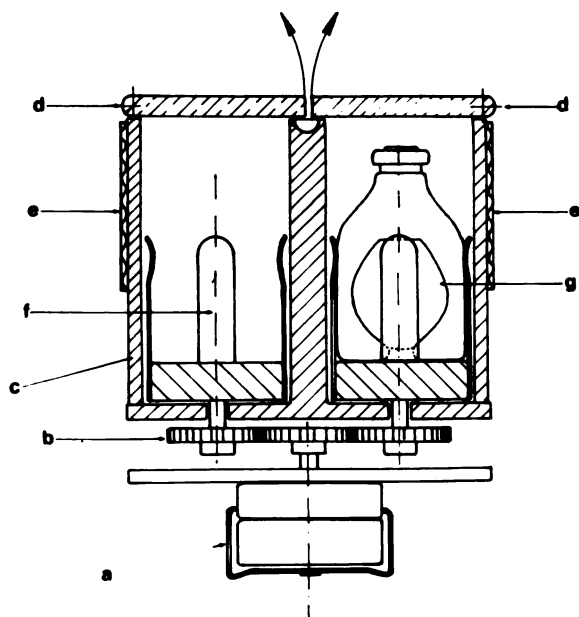


Fig. 2. View of the tonometer

(a) Stirring motor; (b) transmission gears; (c) aluminum block; (d) Perspex covers (shown closed in the figure); (e) 15-W heating elements; (f) aluminum holders for flasks; (g) 0.25 mL-sample flask. The assembly for the small flasks only is shown

both having been dried by passage through a silica gel column (oxygen content 0.00 and 20.96 mL/100 mL, respectively).

**Preparation of flasks.** Figure 3 shows a schematic diagram of the arrangement of the apparatus. Gases from two high-pressure cylinders (A and B) with the same CO<sub>2</sub> content are mixed in E. The relative partition of gases is regulated by the two flowmeters, C and D, above which the pressure of gas is held at 2 atm, in order to attain the required stability of flow rate. A 20 × 0.5 cm, i.d., Pyrex tubing (F) is filled with glass wool to assure complete mixing of gases. A small portion of gas is diverted (G) and continuously sampled for the oxygen content analysis. The remaining portion flows through a larger distribution flask (H) to the tonometric flasks (I) and to a 100-mL cylinder (L) filled with water. Two needles, 0.90-mm gauge, are inserted into each vial for the influx and efflux of gas. Bubbling gas in the cylinder (L) is useful for visually checking that the gas flow through the system is correct and for adjusting the pressure in the flasks when disconnecting them at the end of the appropriate time interval.

We use the following procedure to avoid excessive positive pressure inside the flasks. First raise the efflux needle (submerged in flask L) to the edge of the water level, whereupon the pressure in the flask becomes the same as the atmospheric pressure, then disconnect the influx needle. The flask can be washed by passing through it a large excess of gas. This operation takes about 4 min for a gas flow of 200 mL/min.

**Blood samples.** To obtain the data for the nomogram reported in this paper, we performed 63 determinations of  $p_{50}$  on fresh heparinized samples of blood from two healthy, nonsmoking donors (MS and AM). The samples had virtually the same blood oxygen affinity. A total of 15–20 mL of whole blood was used. All the experiments at a preset concentration of 2,3-DPG and ATP were carried out within 4 to 5 h after venipuncture or after the blood was prepared for analysis. During this time interval the sample was kept at 2 °C.

To determine the Bohr effect, we varied the pH of the sample by injecting 1 to 5 μL of either 2.0 or 0.4 mol/L lactic acid, or 1 mol/L NaHCO<sub>3</sub>, before the blood was added. We used titration curves run on separate samples to calculate the amount of acid or base required to obtain the required pH

value at each  $p_{CO_2}$ . The 2,3-DPG content was altered in vitro according to Dueticke et al. (6) and Samaja and Winslow (7).

**Tonometry of blood.** Tonometric flasks were loaded into the tonometer after the sample was injected into them. In spite of the relatively poor thermal conductivity of Pyrex, we found that the temperature of the flasks reached equilibrium in about 7 to 9 min. Temperature drifts, as measured with a thermal sensor during the tonometry, never exceeded 0.1 °C. After tonometry, flasks were opened while upright and blood was sampled from the bottom with a 10-μL pipettor for the following measurements.

**Measurement on equilibrated blood.** pH,  $s_{O_2}$ , and organic phosphates were measured in the equilibrated blood. The pH was measured with a pH meter (Model 213; Instrumentation Laboratory, Lexington, MA 02173) calibrated with standard buffers at pH 6.840 and 7.384 at 37.0 °C. Blood  $s_{O_2}$  (saturation with oxygen) was measured with a Micro Blood analyzer (Carlo Erba Strumentazione, Milan, Italy), calibrated as already described (8). Kits for use in the assay of 2,3-DPG and ATP were purchased from Boehringer Biochemia srl, Milan. Calibration curves were drawn from data obtained for purified reagents purchased as the pentacyclohexylammonium salt and the disodium salt, respectively.

**Gas pressures in equilibrated blood.** The  $p_{O_2}$  of the blood sample after equilibration is not the same as that in the flask, because some oxygen is injected into the flask with the oxygenated blood and the blood consumes finite amounts of oxygen in its normal metabolism. A new partition of oxygen among hemoglobin/plasma/gas is therefore established as equilibrium is reached. The corrected  $p_{O_2}$  depends on the oxygen affinity of hemoglobin, the hemoglobin concentration, the solubility of oxygen in plasma, the volume of the flask, the volume of blood, and the temperature. The quantitation of these factors is given in Appendix A. Similarly, calculation of the final  $p_{CO_2}$  in the flask after tonometry is given in Appendix A. An estimation of the decrease in  $p_{CO_2}$  is also provided by Figure 4.

**Calculation of  $p_{50}$ .** The value of  $p_{50}$  as a function of  $p_{O_2}$  and  $s_{O_2}$  is calculated from Hill's transformation, which is approximately valid in the range 30 to 70%  $s_{O_2}$ , by using a Hill factor (n) of 2.7 (9) for human normal blood:

$$\log p_{50} = \log p_{O_2} + [\log (s_{O_2}/(100 - s_{O_2}))/n] \quad (1)$$

To obtain values for normal blood, we measured  $p_{50}$ , [2,3-DPG]/[Hb<sub>4</sub>], and pH in fresh heparinized blood from 17

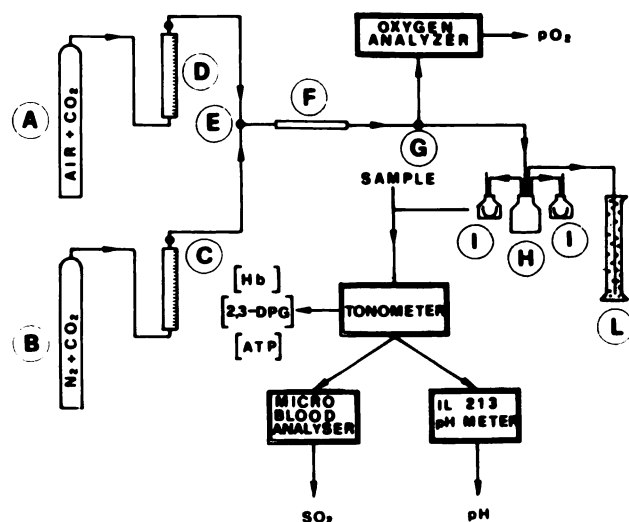


Fig. 3. Simplified diagram representing the experimental procedure

See text for explanations of diagram

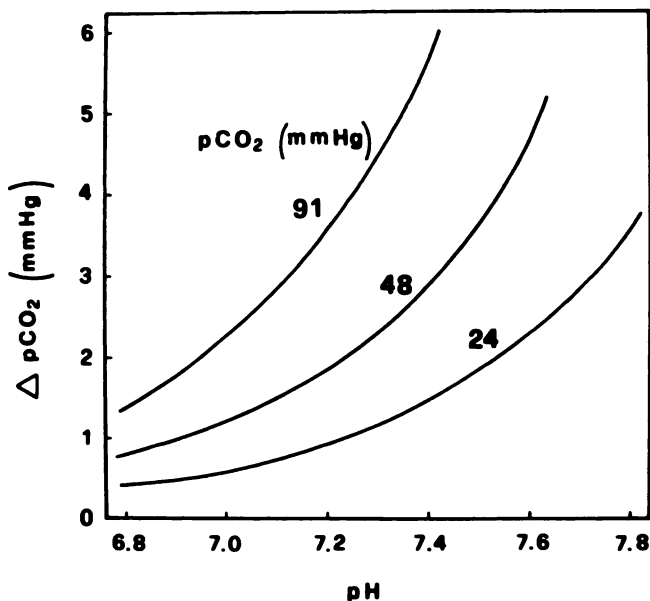


Fig. 4. Decrease of  $p_{CO_2}$  in the flask (considered as a closed system with a volume of 43 mL) after addition of 0.25 mL of  $CO_2$ -free blood, as a function of pH and  $p_{CO_2}$

nonsmoking healthy volunteers of both sexes at  $p_{CO_2} = 48$  mmHg, within 1 h of venipuncture.

## Results

**Reproducibility.** Table 1 shows the reproducibility of the blood values as measured for a single sample.

**Bohr effect.** When we determined the  $p_{50}$ , most of the  $s_{O_2}$  values fell within the range 45 to 55%. In those experiments in which  $s_{O_2}$  was outside this range, the gas concentration in the flask was adjusted appropriately and the measurement was repeated. To evaluate the Bohr effect for each set of conditions of  $p_{CO_2}$  and  $[2,3\text{-DPG}]/[\text{Hb}_4]$ , we made at least four to six determinations of  $p_{50}$  at different pH values and calculated a linear regression of  $\log p_{50}$  vs pH in the pH range 7.0 to 7.6.  $\log p_{50}$  vs pH always yielded straight lines with correlation coefficients between 0.996 and 1.000.

**Organic phosphates.** We determined the concentrations of 2,3-DPG and ATP several times during the experiments and found them to be practically unchanged for at least 12 h when blood was stored in crushed ice. The concentration of ATP was found to be almost insensitive to the procedures applied for the depletion and the increase of 2,3-DPG, except for very low 2,3-DPG concentrations (Figure 5). The 2,3-DPG concentration in blood stored in the ice bath differed slightly from that in the sample after tonometry. A mean decrease of 4% in the tonometered sample was observed, regardless of the oxygenation state of hemoglobin and pH. This drawback was eliminated by determining 2,3-DPG and ATP concentrations in the sample after tonometry.

The  $p_{50}$  increases with increasing concentrations of 2,3-DPG (Figure 6), more markedly so at low concentrations of organic phosphate and low plasma pH. When intracellular pH ( $pH_i$ ) instead of plasma pH ( $pH_e$ ) is considered, the increase

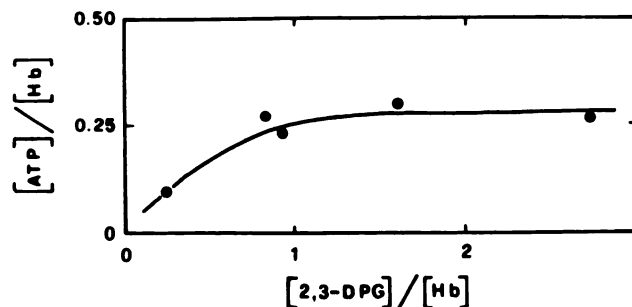


Fig. 5. The concentration of ATP is practically unchanged except at low concentrations of 2,3-DPG, under all the experimental conditions

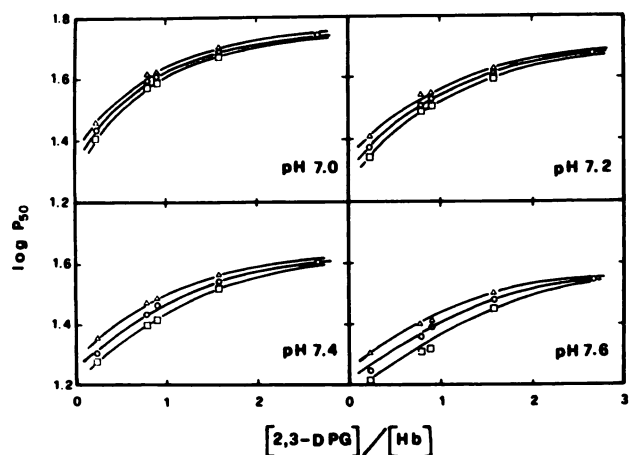


Fig. 6.  $\log p_{50}$  vs  $[2,3\text{-DPG}]/[\text{Hb}_4]$  at four different pH values and three different  $p_{CO_2}$  values (91, 48, and 24 mmHg)

in  $\log p_{50}$  is abolished for  $[2,3\text{-DPG}]/[\text{Hb}_4]$  values  $>1$  (not shown), thus confirming previously reported results (7).

**Equations and nomogram.** The empirical equations reported in Appendix B, derived from Figure 6, allow the calculation of  $p_{50}$  from known  $p_{CO_2}$ , pH, and  $[2,3\text{-DPG}]/[\text{Hb}_4]$  values with an SD of 0.73 mmHg. Figure 7 shows a graphical representation that allows the estimation of  $p_{50}$  with an SD of 0.86 mmHg. The nomogram also allows one to construct the oxyhemoglobin equilibrium curve in the range 10 to 90%, as calculated on the basis of Adair's equation and Adair's constants reported by Winslow et al. (10).

## Discussion

The present method for determination of  $p_{50}$  in whole blood is simple and accurate enough for use in physiological and clinical studies. The use of closed tonometry flasks is advantageous because only small sample volumes are required. Furthermore, the flasks can be filled before the blood is sampled, and the sealed flasks can be stored because their gas composition will remain virtually unchanged for at least six weeks.

The calculations shown in Appendix A and Figure 4 show that the values of  $p_{O_2}$  and  $p_{CO_2}$  at equilibrium can be easily

Table 1. Reproducibility of Data in a Typical Experiment

	$s_{O_2}$ %	pH	[Hb] g/L	$p_{50}$ mmHg	$[2,3\text{-DPG}]$ mmol/L	[ATP]
n	10	10	10	10	4	4
Mean	54.41	7.371	164.0	27.54	2.14	0.87
SD	0.61	0.006	1.6	0.33	0.03	0.03
CV, %	1.1	0.1	1.0	1.2	1.4	3.4

$$\text{REF. } \frac{[2,3\text{-DPG}]}{[\text{Hb}_4]}$$

6

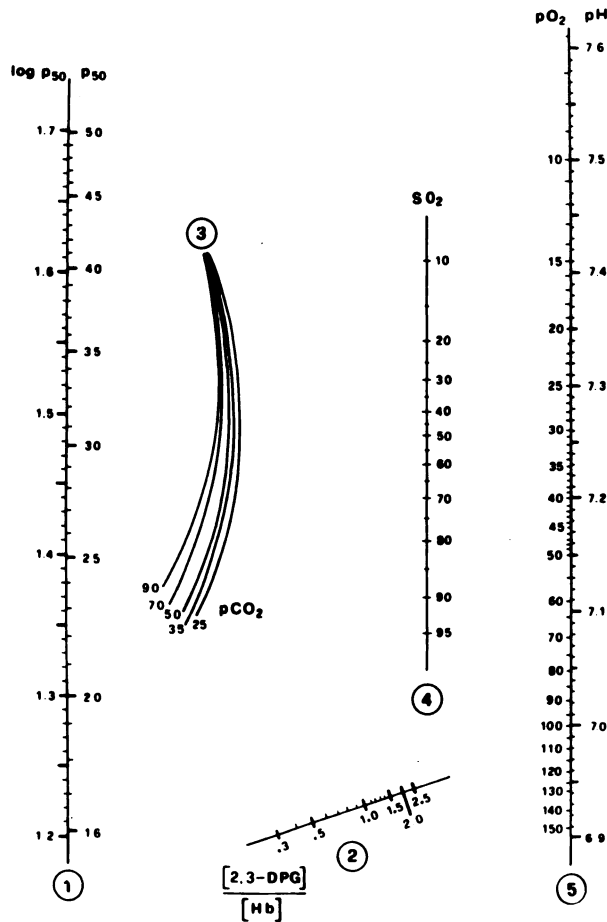


Fig. 7. Nomogram relating  $p_{\text{O}_2}$ ,  $s_{\text{O}_2}$ , pH,  $p_{\text{CO}_2}$ ,  $p_{50}$ , and the  $[2,3\text{-DPG}]/[\text{Hb}_4]$  molar ratio in human blood at  $37.0^\circ\text{C}$

See Appendix C for details; standard errors and explanations are in the text

determined. The oxygen consumption and the carbon dioxide production by the erythrocyte during equilibrium are too small to affect the precise determination of the gas pressures in the flask.

A possible error in the determination of  $p_{50}$  is represented by Hill's factor in equation 1, which we considered to be constant for all the experiments. We assumed a value of  $n = 2.7$ , as already reported (9) and as we confirmed by a separate set of experiments. If, for example,  $s_{\text{O}_2}$  is 40% at a  $p_{\text{O}_2}$  of 23.92 mmHg, the resulting  $p_{50}$  is 27.96 or 27.80 for Hill's factor values of 2.6 and 2.7, respectively. The discrepancy is still less for  $s_{\text{O}_2}$  values approaching 50%. Thus, when  $s_{\text{O}_2}$  is in the range of 40 to 60%, an error in Hill's factor has very little effect on the calculated value for  $p_{50}$ . Furthermore, Hill's factor is constant under various conditions of pH and  $[2,3\text{-DPG}]/[\text{Hb}_4]$  (7).

Table 2 shows the influence on  $p_{50}$  of errors in the various measured variables. Clearly, the most critical variable is the concentration of 2,3-DPG.

Since the early discovery that 2,3-DPG is a potent factor for the reduction of the oxygen affinity of human hemoglobin (11), several other organic and inorganic phosphates have been found to have similar effects in vitro (12). However, in human erythrocytes, only 2,3-DPG and ATP are present in sufficient

Table 2. Error Analysis of the Described Method

Size of error	Error component	Change in $p_{50}$ , mmHg
1.0%	$s_{\text{O}_2}$	0.40
0.01%	$[\text{O}_2]$ , %	0.08
0.01	pH	0.20 <sup>a</sup>
0.1	$[2,3\text{-DPG}]/[\text{Hb}]$	1.11 <sup>b</sup>
0.1	$n$ (Hill)	0.16 <sup>c</sup>

<sup>a</sup> Assuming a Bohr factor of  $-0.40$ . <sup>b</sup> At  $[2,3\text{-DPG}]/[\text{Hb}_4] = 1.0$ . <sup>c</sup> At  $p_{\text{O}_2} = 24$  mmHg and  $s_{\text{O}_2} = 40\%$ .

quantity to influence the oxygen affinity of blood (13). The concomitant presence in human erythrocytes of a divalent cation such as  $\text{Mg}^{2+}$ , which binds to ATP to form an unreactive  $\text{Mg-ATP}$  complex (13-15), minimizes the allosteric effect of ATP on human hemoglobin. However, unreactive ATP is still expected to have some influence on  $p_{50}$  when mediated via  $\text{pH}_i$ , similar to that of 2,3-DPG when present in saturating amounts (7), because ATP is also negatively charged at physiological  $\text{pH}_i$ . Figure 5 shows that ATP concentration changes are very small under most of the conditions we studied. Moreover, the fraction of organic phosphates bound to  $\text{Mg}^{2+}$  (and thus less effective in decreasing  $\text{pH}_i$ , because the  $\text{Mg-ATP}$  complex has only two negative charges) is much greater for ATP than for 2,3-DPG, because 70 to 80% of erythrocyte ATP is bound to  $\text{Mg}^{2+}$  (13). All these observations led us to exclude ATP concentrations from our computations.

Calculation of  $p_{50}$  from a single measurement of  $p_{\text{O}_2}$ ,  $s_{\text{O}_2}$ , pH, and  $[2,3\text{-DPG}]/[\text{Hb}_4]$  can be very advantageous because these variables can be easily measured and do not require special techniques; they can also be determined in vivo. The nomogram of Figure 7 was drawn according to the previously reported model (5). The main difference consists in the non-linearity of the iso- $p_{\text{CO}_2}$  lines, probably because in the present work we considered a wider range of values for  $[2,3\text{-DPG}]/[\text{Hb}_4]$ .

The correlation between the experimentally determined  $p_{50}$  and that calculated from the nomogram and from the equations is shown in Figure 8. Precision is slightly improved if the equations reported in Appendix B are used ( $r = 0.9938$  and  $0.9853$ , respectively). In this case, the scattering of the data is almost constant over the entire range, whereas data obtained from the nomogram, although more scattered in the central portion, are more accurate at the lower and upper extremes.

The difference between experimental values for  $p_{50}$  as determined on normal subjects, 10 men and seven women, at known values of  $p_{\text{CO}_2}$ , pH, and  $[2,3\text{-DPG}]/[\text{Hb}_4]$ , and the value of  $p_{50}$  calculated from the equations reported in Appendix B was  $0.37 \pm 0.80$  mmHg, i.e., within the experimental error of the measurements. This confirms on a more limited range the conclusions drawn from the extensive study on the two normal subjects reported in this paper. The nomogram and the equations are not valid for temperatures other than  $37^\circ\text{C}$ , for abnormal hemoglobins, and, more generally, for any of the conditions that induce a change in Bohr's or Hill's factor.

The nomogram can also be used in a reverse mode, i.e., to calculate  $[2,3\text{-DPG}]/[\text{Hb}_4]$  from known  $p_{50}$ ,  $p_{\text{CO}_2}$ , and pH. An SD of  $0.12 [2,3\text{-DPG}]/[\text{Hb}_4]$  units ( $n = 58$ ) was found in this case. The equations may also be rearranged so that  $[2,3\text{-DPG}]/[\text{Hb}_4]$  is the dependent variable and all the others are the independent variables.

The operators must be warned that line 4 and the left side of line 5 of Figure 7 are determined by assuming a  $[2,3\text{-DPG}]/[\text{Hb}_4]$  of 0.8, a  $p_{\text{CO}_2}$  of 40 mmHg, and a pH of 7.4. Although characterization of the oxyhemoglobin equilibrium

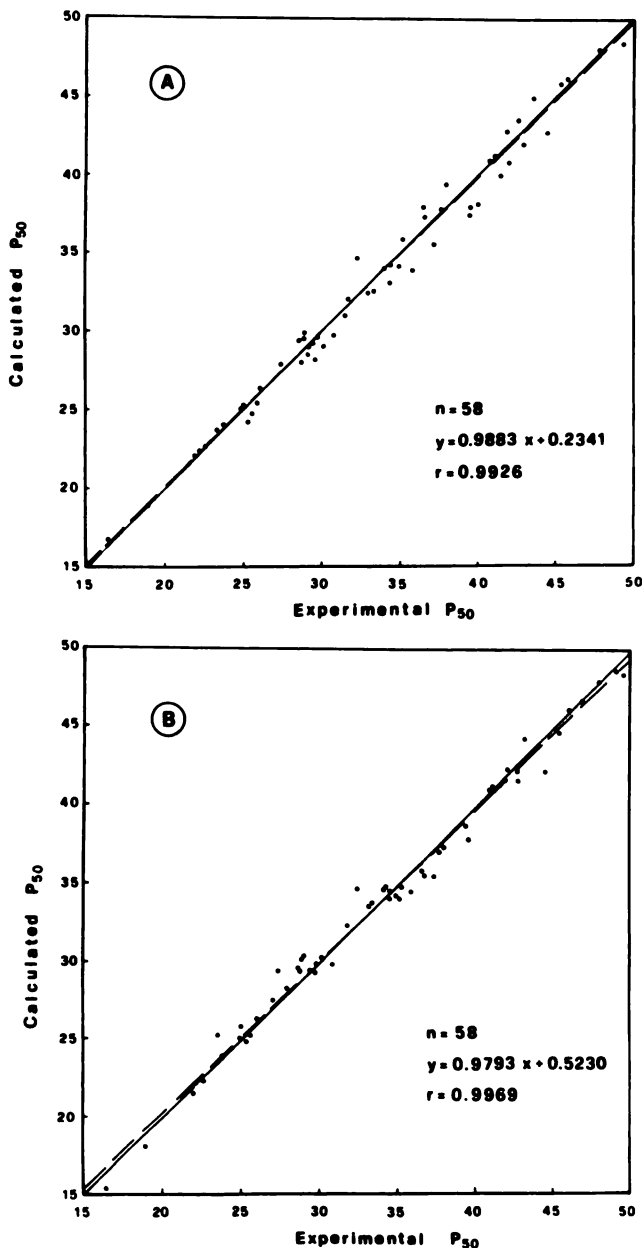


Fig. 8. Correlation between the experimental  $p_{50}$  and the  $p_{50}$  derived from the nomogram (A) or from the equations (B). A few experiments with  $p_{50}$  values beyond the 15 to 50 mmHg range are not reported in the Figure. Results of least-squares regression analyses are shown.

curve by Hill's equation does not account for changes in shape under various conditions of pH and  $[2,3\text{-DPG}]/[\text{Hb}_4]$ , the four Adair parameters are sensitive to these effects. We therefore discourage the calculations of  $p_{50}$  from known  $p_{\text{O}_2}$  and  $s_{\text{O}_2}$ . More work is in progress to correlate not only the position but also the shape of the oxyhemoglobin equilibrium curve to the values of pH,  $p_{\text{CO}_2}$ , and  $[2,3\text{-DPG}]/[\text{Hb}_4]$ .

This study was supported by grant no. 79.03250.04 from the Consiglio Nazionale delle Ricerche, Rome.

### Appendix A

The calculation of the  $p_{\text{O}_2}$  (mmHg) from the  $\text{O}_2$  content (mL/100 mL) of the gas phase is by the formula:

$$p_{\text{O}_2} = (\text{O}_2 \times \text{BP}) / 100 \quad (\text{A1})$$

where BP is the barometric pressure. The obtained  $p_{\text{O}_2}$  does

not correspond to the actual  $p_{\text{O}_2}$  in the flask, and the following corrections must apply.

The first is necessary because the flasks, although washed with gas at room temperature  $t$  ( $^{\circ}\text{C}$ ), are tonometered at  $37^{\circ}\text{C}$ :

$$p_{\text{O}_2,37^{\circ}\text{C}} = p_{\text{O}_2,t} \times (273 + 37)/(273 + t) \quad (\text{A2})$$

A second correction compensates for the increase in total pressure due to the addition of an incompressible liquid in a closed system. If the flask and sample volumes are defined as  $V_f$  and  $V_s$ , respectively, then:

$$p_{\text{O}_2} = p_{\text{O}_2} \times [V_f / (V_f - V_s)] \quad (\text{A3})$$

A third correction accounts for the oxygen dissolved in the sample, which alters the original composition of gas. The following formula relates  $p_{\text{O}_2}$  with the hemoglobin concentration (g/L) in the sample, its  $s_{\text{O}_2}$  before tonometry ( $s_{\text{O}_2,\text{in}}$ ), final  $s_{\text{O}_2}$  ( $s_{\text{O}_2,\text{fin}}$ ), temperature ( $t$ ), and the volume of the sample ( $V_s$ ):

$$p_{\text{O}_2} = p_{\text{O}_2} + [(s_{\text{O}_2,\text{in}} - s_{\text{O}_2,\text{fin}})/(s_{\text{O}_2,\text{in}})] \times [\text{Hb}] \times V_s \times \text{BP} \times (273 + t) \times 1.213 \times 10^{-4} \quad (\text{A4})$$

Under standard conditions (room temperature  $23^{\circ}\text{C}$ , barometric pressure 760 mmHg, standard sample volumes) all the above corrections (equations A1 to A4) reduce to

$$p_{\text{O}_2} = (\text{O}_2 \times 8.007) + [[\text{Hb}] \times (s_{\text{O}_2,\text{in}} - s_{\text{O}_2,\text{fin}})/14\ 654] \quad (\text{A5})$$

for small flasks, and to

$$p_{\text{O}_2} = (\text{O}_2 \times 8.008) + [[\text{Hb}] \times (s_{\text{O}_2,\text{in}} - s_{\text{O}_2,\text{fin}})/13\ 930] \quad (\text{A6})$$

for large flasks.

The oxygen consumption due to the metabolic needs of the erythrocytes has been calculated to be  $<0.09$  mmHg over a period of 30 min at a  $p_{\text{O}_2}$  of 150 mmHg (*Documenta Geigy, Tables Scientifiques*, Ciba-Geigy, SA, Basle, Swiss ed., 7th ed., p 627).

When blood is injected into the flask, part of the gaseous  $\text{CO}_2$  dissolves in the liquid phase and is hydrated to give bicarbonate ions. At a given  $p_{\text{CO}_2}$  and pH, the total  $\text{CO}_2$  content in the liquid phase is calculated from the Siggaard-Andersen alignment nomogram (O. Siggaard-Andersen, In *The Acid-Base Status of Blood*, Munksgaard, Copenhagen, 1974). The new  $p_{\text{CO}_2}$  is then calculated accordingly. Figure 4 represents a standard case, i.e., flask volume 43 mL and sample volume 0.25 mL. Very small changes ( $<0.2$  mmHg) are expected in other practical cases.

The increase in  $p_{\text{CO}_2}$  during the period of tonometry related to the  $\text{CO}_2$  produced by the cells for the metabolism was calculated to be 0.08 mmHg at a  $p_{\text{CO}_2}$  of 40 mmHg.

### Appendix B

Data points from Figure 6 can be fitted to an empirical equation of the form

$$\log p_{50} = a \times \log ([2,3\text{-DPG}]/[\text{Hb}_4]) + b \quad (\text{B1})$$

by the least-squares regression analysis, with a mean chi-square residual of 0.004  $\log p_{50}$  units. Parameters  $a$  and  $b$  from equation B1 are linear functions of  $p_{\text{CO}_2}$  (5) and therefore can be fitted to an equation of the form:

$$(a \text{ or } b) = c \times p_{\text{CO}_2} + d \quad (\text{B2})$$

Assigning appropriate values to  $c$  and  $d$  and substituting equation B2 in equation B1,  $\log p_{50}$  can be estimated from known values of  $p_{\text{CO}_2}$  and the  $[2,3\text{-DPG}]/[\text{Hb}_4]$  molar ratio, at a definite value of pH. The most probable values for  $c$  and

d were determined at the two extreme pH values, 7.0 and 7.6:

$$\log p_{50(7.0)} = (-0.69117 \times 10^{-3} \times P + 0.3365)G + (0.3598 \times 10^{-3} \times P + 1.599) \quad (B3)$$

$$\log p_{50(7.6)} = (-0.1380 \times 10^{-2} \times P + 0.3607)G + (0.9089 \times 10^{-3} \times P + 1.360) \quad (B4)$$

where G is  $\log [2,3\text{-DPG}]/[\text{Hb}]$ , and P is the  $p_{\text{CO}_2}$ .

Because  $\log p_{50}$  is always a linear function of pH in the range 6.9 to 7.6, its value at any pH in this range can be interpolated by use of the following formula:

$$\log p_{50(\text{pH})} = \{(\text{pH} - 7.0) \times (\log p_{50(7.6)} - \log p_{50(7.0)})\} / 0.6 + \log p_{50(7.0)} \quad (B5)$$

This empirical relationship allows the estimation of  $p_{50}$  at any given pH (range 6.9 to 7.6),  $p_{\text{CO}_2}$  (range 20 to 90 mmHg), and  $[2,3\text{-DPG}]/[\text{Hb}_4]$  ratio (range 0.3 to 2.5), with 0.73 mmHg SD.

## Appendix C

To construct the nomogram, two parallel lines (1 and 5) were traced and  $\log p_{50}$  and pH were expressed linearly. Then the loci of intersection of all the values of pH and  $\log p_{50}$  at constant  $p_{\text{CO}_2}$  and  $[2,3\text{-DPG}]/[\text{Hb}_4]$  were defined. A continuous linear relationship was found between all  $[2,3\text{-DPG}]/[\text{Hb}_4]$  values. In contrast,  $p_{\text{CO}_2}$  values followed a curvilinear relationship; thus only a few iso- $p_{\text{CO}_2}$  lines have been reported (3). Line 4 and the left side of line 5 report values referring to the oxyhemoglobin equilibrium curve, as outlined in the text.

The use of the nomogram can be better understood from the following examples.

**Example 1.** Given a blood sample with  $p_{\text{CO}_2} = 50$  mmHg, pH 7.4,  $[2,3\text{-DPG}]/[\text{Hb}_4] = 0.9$ , calculate the  $p_{50}$  and  $s_{\text{O}_2}$  at  $p_{\text{O}_2} = 41$  mmHg. Connect REF  $[2,3\text{-DPG}]/[\text{Hb}_4]$  (point 6) to 0.9 on line 2. Mark the crossing point between this line and the iso- $p_{\text{CO}_2}$  line at  $p_{\text{CO}_2} = 50$ . Connect this point to pH 7.4, line 5, and extrapolate to line 1;  $p_{50}$  is 28.2 mmHg. Connect this value to  $p_{\text{O}_2} = 41$ , line 5. The intersection with line 4 is the  $s_{\text{O}_2}$  at  $p_{\text{O}_2} = 41$  mmHg and  $p_{50} = 28.2$  mmHg.

**Example 2.** Given a blood sample with a known  $p_{50}$  of 25 mmHg at pH 7.2 and  $p_{\text{CO}_2} = 70$  mmHg, calculate its  $[2,3\text{-DPG}]/[\text{Hb}_4]$  value. Connect 25, line 1, to 7.2, line 5, and mark the crossing point of this line with the iso- $p_{\text{CO}_2}$  70 mmHg line. Connect this point to REF  $[2,3\text{-DPG}]/[\text{Hb}_4]$  and extrapolate to line 5; the  $[2,3\text{-DPG}]/[\text{Hb}_4]$  ratio is about 0.3.

## References

- Severinghaus, J. W., Blood gas calculator. *J. Appl. Physiol.* **21**, 1108-1116 (1966).
- Aberman, A., Cavanilles, J. M., and Weil, M. H., Blood  $p_{50}$  calculated from a single measurement of pH,  $p_{\text{O}_2}$ , and  $s_{\text{O}_2}$ . *J. Appl. Physiol.* **38**, 171-176 (1975).
- Tien, Y. K., and Gabel, R. A., Prediction of  $p_{\text{O}_2}$  and  $s_{\text{O}_2}$  using the standard oxygen hemoglobin equilibrium curve. *J. Appl. Physiol.* **42**, 985-987 (1977).
- Severinghaus, J. W., Simple, accurate equations for human blood  $\text{O}_2$  dissociation computations. *J. Appl. Physiol.* **46**, 599-602 (1979).
- Musetti, A., Rossi, F., and Rossi-Bernardi, L., The  $\log p_{50}$  and oxygen dissociation curve nomogram for human blood at 37 °C. In *Physiological Basis of Anesthesiology*, W. W. Mushin, Ed., Piccin, Padova, Italy, 1975, pp 95-110.
- Deuticke, B., Duhm, J., and Dierkesmann, R., Maximal elevation of 2,3-diphosphoglycerate concentration in human erythrocytes: Influence on glycolytic metabolism and intracellular pH. *Pfluegers Arch.* **326**, 15-34 (1971).
- Samaja, M., and Winslow, R. M., The separate effect of  $\text{H}^+$  and 2,3-DPG on the oxygen equilibrium curve of human blood. *Br. J. Haematol.* **41**, 373-381 (1979).
- Rossi-Bernardi, L., Perrella, M., Luzzana, M., et al. Simultaneous determination of the hemoglobin derivatives, oxygen content, and oxygen saturation in 10  $\mu\text{L}$  of whole blood. *Clin. Chem.* **23**, 1215-1225 (1977).
- Roughton, F. J. W., Transport of oxygen and carbon dioxide. In *Handbook of Physiology Section 3*, Vol. 1, W. O. Fenn and H. Rohn, Eds., American Physiological Society, Washington, DC, 1964, pp 767-825.
- Winslow, R. M., Swenberg, M. L., Berger, R. L., et al. Oxygen equilibrium curve of normal human blood and its evaluation by Adair's equation. *J. Biol. Chem.* **252**, 2331-2337 (1977).
- Benesch, R., Benesch, R. E., and Yu, C. I. Reciprocal binding of oxygen and diphosphoglycerate by human hemoglobin. *Proc. Natl. Acad. Sci. USA* **59**, 526-532 (1967).
- Chanutin, A., and Curnish, R. R., Effects of organic and inorganic phosphates on the oxygen equilibrium of human erythrocytes. *Arch. Biochem. Biophys.* **121**, 96-102 (1967).
- Bunn, H. F., Ransil, B. J., and Chao, A., The interaction between erythrocyte organic phosphates, magnesium ion and hemoglobin. *J. Biol. Chem.* **246**, 5273-5279 (1971).
- Berger, H., Janig, G. R., Gerber, G., et al., Interaction of hemoglobin with ions. Interaction among magnesium, adenosine-5'-triphosphate, 2,3-diphosphoglycerate and oxygenated and deoxygenated human hemoglobin under simulated intracellular conditions. *Eur. J. Biochem.* **38**, 553-562 (1973).
- Gerber, G., Berger, H., Janig, G. R., and Rapoport, S. M., Interactions of hemoglobin with ions. Quantitative description of the state of magnesium, adenosine-5'-triphosphate, and 2,3-diphosphoglycerate in human hemoglobin under simulated intracellular conditions. *Eur. J. Biochem.* **38**, 563-571 (1973).